# Self-Assembled Monolayers from Biphenyldithiol Derivatives: Optimization of the Deprotection Procedure and Effect of the Molecular Conformation

**Andrey Shaporenko,[†] Mark Elbing,[‡] Alfred Błaszczyk,[‡,§] Carsten von Hänisch,[‡] Marcel Mayor,*[,‡,||] and Michael Zharnikov*[,†]**

*Angewandte Physikalische Chemie, Universität Heidelberg, Im Neuenheimer Feld 253, 69120 Heidelberg, Germany, Forschungszentrum Karlsruhe GmbH, Institute for Nanotechnology, P.O. Box 3640, 76021 Karlsruhe, Germany, Faculty of Commodity Science, Al. Niepodległości 10, 60-967 Poznań, Poland, and Department of Chemistry, University of Basel, St. Johannsring 19, CH-4056 Basel, Switzerland*

*Received: November 24, 2005; In Final Form: January 5, 2006*

A series of biphenyl-derived dithiol (BDDT) compounds with terminal acetyl-protected sulfur groups and different structural arrangements of both phenyl rings have been synthesized and fully characterized. The different arrangements were achieved by introducing hydrocarbon substituents in the 2 and 2′ positions of the biphenyl backbone. The presented model compounds enable the investigation of the correlation between the intramolecular conformation and other physical properties of interest, like, e.g., molecular assembly or electronic transport properties. Here, the ability of these model compounds to form self-assembled monolayers (SAMs) on Au(111) and Ag(111) is investigated in details. The deprotection of the target molecules was performed in situ using either $NH_4OH$ or triethylamine (TEA) deprotection agent. The fabricated films were characterized by synchrotron-based high-resolution photoelectron spectroscopy and near-edge absorption fine structure spectroscopy. Whereas the deprotection by $NH_4OH$ was found to result in the formation of multilayer films, the deprotection by TEA allowed the preparation of densely packed BDDT SAMs with a noticeably higher orientational order and smaller molecular inclination on Ag than on Au. Introduction of the alkyl bridge between the individual rings of the biphenyl backbone did not lead to a noticeable change in the structure and packing density of the BDDT SAMs as long as the molecule had a planar conformation in the respective SAM. The deviation from this conformation resulted in the deterioration of the film quality and a decrease of the orientational order.

## 1. Introduction

The ongoing miniaturization of silicon-based electronic technology will reach its physical limit in the foreseeable future,[1] and hence, alternative concepts that allow further reducing the size of electronic active components are highly desirable. In particular, the concept of molecular electronics[2,3] that envisages the use of molecular structures to build electronic devices has received considerable scientific as well as popular interest recently.[4−6] Although contacting few organic molecules or even single molecules still remains a difficult task, significant advances in manipulation on the nanoscale over the past years resulted in a number of different protocols to form metal−molecule−metal junctions.[7,8] Examples of different test devices used are crossed-wire junctions,[9] mercury drop electrodes,[10] atomic force microscopy,[11] scanning tunneling microscopy,[12] and mechanically controlled break junctions.[13] The electronic properties of the metal−molecule−metal junctions indeed depend on the molecular structure, as demonstrated recently by a single molecule immobilized in a break junction displaying the characteristics of a rectifier.[14] However, not all parameters of the junctions are understood accurately enough up to now to predict the electronic properties of a molecular contact solely based on the knowledge of the molecular structure. The structure of the organic molecule is only one aspect that influences the electronic response, while other factors seem to be of importance as well. In fact, sometimes the same molecule gives rise to different *I*/*V* curves in different setups.[15,16] The coupling between the molecule and the electrodes, i.e., the nature of the interface,[17−19] may provide one possible explanation for differing results in two distinct setups. In the majority of test devices to record current−voltage (*I*/*V*) characteristics of organic molecules the studied molecule is self-assembled on at least one metal surface, i.e., one electrode. In fact, often a self-assembled monolayer (SAM) of the organic molecule forms an integral part of the device. Usually, the SAM is formed by reaction between an organic thiol and a metal surface, mostly gold, providing at least one interface. The coupling to the second electrode differs depending on the setup. In addition to the interface, also the orientation and arrangement of the monolayer on the electrode surface probably play an important role for the characteristics of the junction.[20] Unfortunately, at present, the structure of SAMs has been mainly studied for simple *n*-alkanethiols,[20−23] which, due to their insulating properties,[10] will probably not give rise to junctions with interesting electronic properties and hardly be used as components of molecular electronic devices. Similar investigations on aromatic compounds, which are more promising candidates for molecular electronic devices, are scarce (see, e.g., refs 24−29). The available data suggests that both the interface and the interactions between neighboring molecules govern the structure of

* Corresponding authors: marcel.mayor@unibas.ch (M. Mayor) and Michael.Zharnikov@urz.uni-heidelberg.de (M. Zharnikov).
[†] Universität Heidelberg.
[‡] Institute for Nanotechnology.
[§] Faculty of Commodity Science.
[||] University of Basel.

10.1021/jp056833z CCC: $33.50 
Published on Web 02/03/2006

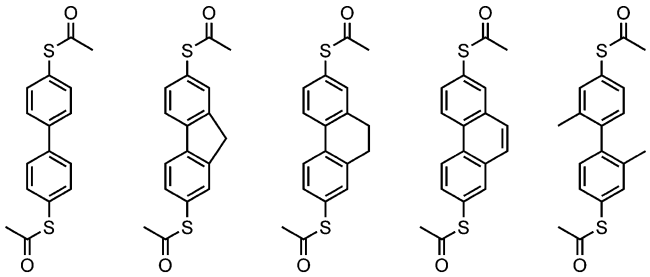

**1** **2** **3** **4** **5**

**Figure 1.** Molecules of this study. Both compounds and respective SAMs are denoted as **1**−**5**.

the SAM. However, based on current knowledge, the structure of the SAM cannot be exactly predicted by looking at the structure of the SAM constituents.

To establish a better correlation between the molecular structure and the properties of the aromatic SAMs with 4′-thiol substitution, we designed and synthesized a series of biphenyl-based dithiols (BBDT) with acetyl-protected thiol groups and different conformations of the biphenyl backbone (see Figure 1). The protection is believed to promote the formation of good-quality SAMs, suppress the dimerization, and prevent the multilayer formation.[30,31] This paper is devoted to the characterization of the respective SAMs on evaporated Au(111) and Ag(111) substrates with emphasis on optimization of the deprotection procedure and the influence of the molecular conformation on the structure and packing density of the SAMs.

Starting from the simple biphenyl backbone (**1**), which has a dihedral angle of ∼39° in the molecular state and is assumed to have a planar conformation in the solid state,[32,33] two different kinds of compounds comprising the biphenyl motif have been designed and synthesized (see Figure 1 and Table 1). First, it was envisaged to fix the angle between two adjacent phenyl rings of a biphenyl by introduction of an alkyl bridge in positions 2 and 2′. Whereas no crystals of the respective compounds **2**−**4** that were suitable for X-ray analysis have been obtained to date, crystal structures of the parent compounds, i.e., fluorene, 9,-10-dihydrophenanthrene, and phenanthrene, are known. The fluorene should be essentially planar with a torsion angle between the two phenyl rings of almost 0°. However, the biphenyl backbone is curved due to the large strain induced by the central five-membered ring.[34] X-ray analysis of 9,10-dihydrophenanthrene showed a torsion angle of about 20° between the two phenyl rings.[35] Crystal structure analysis revealed that the phenanthrene moiety is planar.[36]

Furthermore, a nonbridged biphenyl **5** with methyl groups in the ortho position to the ring connecting carbons has been synthesized as a member of a series of oligophenylenes with different length.[37] Due to the steric constrains and repulsion between the methyl moieties, compound **5** should exhibit a considerable dihedral angle in both the molecular and the solid state. Indeed, the solid-state structure of **5** displays a torsion angle of nearly 80° between the planes of both phenyl rings.[37]

Thus far, only SAMs **1** and **2** on Au(111) substrate were investigated. However, reported parameters of these films are quite scarce, and there is a disagreement between the results of different authors. Whereas M. Tour et al.,[30] Kang et al.,[27] and B. de Boer[31] reported the formation of good-quality SAMs **1** and **2**, Azzam et al.[38] concluded that organodithiols with a short oligophenyl backbone, such as, e.g., **1**, do not form well-oriented layers (as shown later,[39] the SAM quality can be noticeably improved by introduction of methylene linkages between the thiol groups and biphenyl moiety). Note, however, that the conclusions on the good quality of SAMs **1** and **2** in refs 27, 30, and 31 were based on the limited data sets and a larger molecular inclination of the SAM constituents as compared to longer *p*-phenylene systems was mentioned. In this study, we used a combination of such powerful methods as synchrotron-based high-resolution photoelectron spectroscopy (HRXPS) and near-edge absorption fine structure (NEXAFS) spectroscopy, which allowed us to characterize the SAMs in detail.

In the following section we describe the experimental procedure and techniques. The results are presented in section 3 followed by a discussion and summary in sections 4 and 5, respectively.

## 2. Experimental Section

**2.1. Synthesis of the Biphenyl Derivatives 1−5.** All chemicals were used as received from the supplier. If not mentioned otherwise, the solvents were p.a. quality and used without further purification. Dry THF was obtained by distillation from a sodium benzophenone slurry according to a literature procedure.[40] Dry DMI was purchased from Fluka. If not mentioned otherwise, all reactions were carried out under an atmosphere of nitrogen or argon. TLC was performed on Merck silica gel 60 $F_{254}$ plates and column chromatography using Merck silica gel 60 (0.040−0.063 mm).

The syntheses of the alkyl-bridged target compounds **2**−**4** are summarized in Scheme 1. Target compound **2** containing only one bridging C atom was prepared starting from commercially available 2,7-dibromofluorene. The two bromines of **6** were substituted using a three-step one-pot protocol that had been developed earlier (in the following called halide-to-thioacetyl conversion).[37] The three steps are as follows: (1) nucleophilic aromatic substitution using sodium methanethiolate in DMI[41] at 120 °C to afford the intermediate (not isolated) compound bearing two terminal SMe groups, (2) nucleophilic cleavage of the thiomethyl groups using a 5-fold excess of sodium methanethiolate and long reaction time at 120 °C,[42] and (3) acetyl protection of the free thiol groups by careful addition of acetyl chloride at room temperature.[43] Using this method, compound **2** has been obtained as a slightly yellow solid in a yield of 43% after column chromatography. Target compound **3** bearing two saturated carbons in the bridge was obtained from 9,10-dihydrophenanthrene **7**. First, iodination following a literature procedure gave compound **8** having iodo groups in positions 2 and 7.[44] Biphenyl **8** was obtained as a white solid in a yield of 56%. The thioacetyl groups were introduced by the halide-to-thioacetyl conversion procedure mentioned above. Target compound **3** having two terminal acetyl-protected sulfur groups was obtained as a white solid in 72% yield after column chromatography. The last member of this series having a fully conjugated $\pi$ system was prepared starting from compound **8**. This was converted to the corresponding phenanthrene using *N*-bromosuccinimide (NBS) and dibenzoylperoxide, affording **9** as a white solid in 84% yield following a known literature procedure.[44] Again, the thioacetyl groups were introduced by the developed halide-to-thioacetyl conversion. Target compound **4** was obtained as a white solid in 63% yield after column chromatography.

The synthetic pathway for the nonbridged biphenyls **1** and **5** is shown in Scheme 2. To obtain target structure **1**, in the first step the two bromines of commercially available 4,4′-dibromobiphenyl **10** were exchanged for *S*-*tert*-butyl groups by a nucleophilic aromatic substitution with sodium *tert*-butyl thiolate in DMI. Purification by column chromatography afforded the

**TABLE 1: Properties of the Molecules of This Study or the Respective Parent Compounds (bond length between the rings should be less than 1.477 Å for good conjugation)[33]**

| | **1** | **2** | **3** | **4** | **5** |
|---|---|---|---|---|---|
| torsion angle according to the molecular simulation | 39° | 0° | 17.5° | 0° | 96° |
| torsion angle in the solid state (**1-4**: for the parent compounds) | 0°[32,33] | 0°[34] | 20°[35] | 0°[36] | 79.7° |
| bond length between the rings (Å) (for the parent compounds) | 1.506[33] | 1.50[34] | | 1.448[36] | 1.487 |

**SCHEME 1: Synthesis of Compounds 2−4**[a]

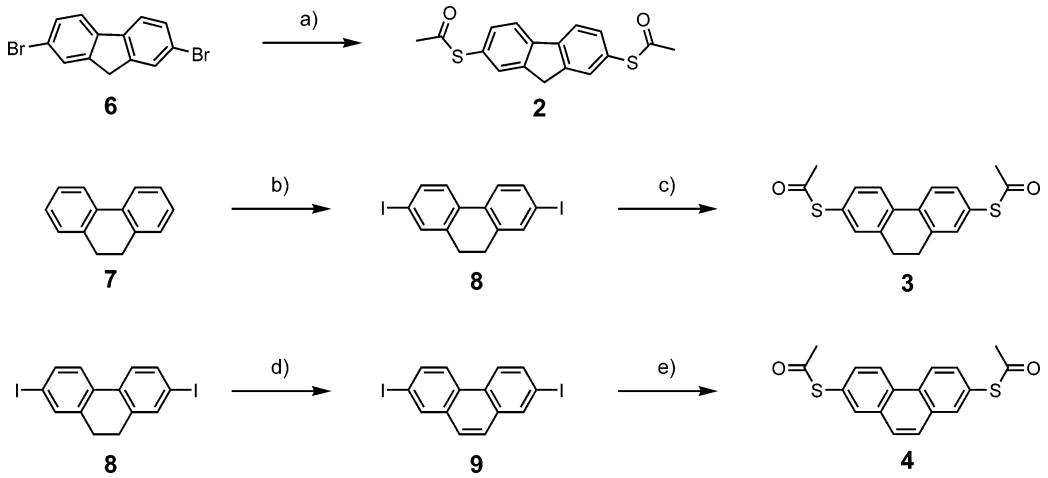


[a] (a) (1,2) NaSMe, DMI, 120 °C, (3) AcCl, DMI, RT, 43%; (b) $I_2$, $HIO_3$, $H_2SO_4$, $CH_3COOH$, $H_2O$, $CCl_4$, 80 °C, 56%; (c) (1,2) NaSMe, DMI, 120 °C, (3) AcCl, DMI, RT, 72%; (d) NBS, $(C_6H_5CO)O_2$, $CCl_4$, RT, 84%; (e) (1,2) NaSMe, DMI, 120 °C, (3) AcCl, DMI, RT, 63%.

**SCHEME 2: Synthesis of Compounds 1 and 5**[a]

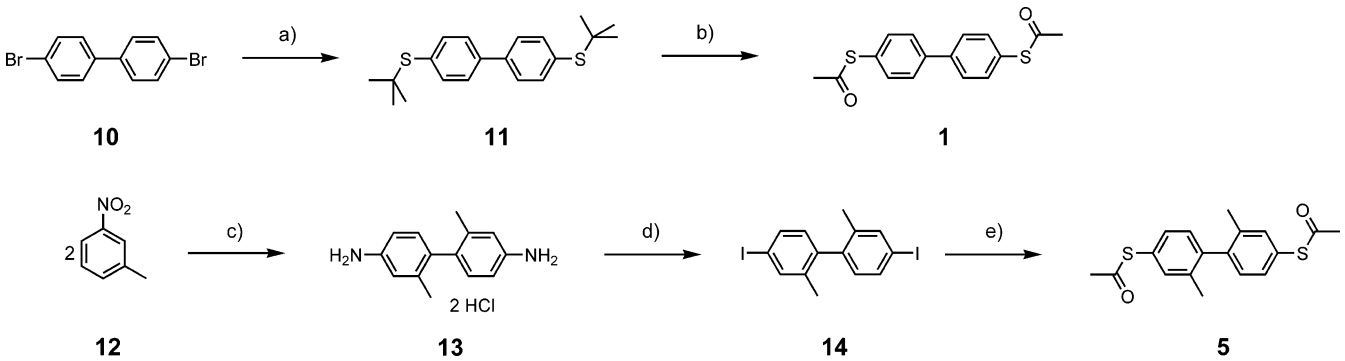


[a] (a) *t*-BuSNa, DMI, 110 °C, 57%; (b) $Br_2$, AcCl, AcOH, RT, 96%; (c) (1) Zn, NaOH, EtOH, RT (2) 20% HCl, EtOH, RF, 55%; (d) (1) 3% $NaNO_2$, 5% $H_2SO_4$, 0 °C, (2) 20% KI, 5% $H_2SO_4$, 70 °C, 67%; (e) (1) *tert.*-BuLi, THF, −78 °C, (2) $S_8$, THF, RT, (3) $Ac_2O$, AcOH, RT, 28%.

desired product **11** as a white solid in a yield of 57%. In the next step, trans protection of the *S-tert*-butyl groups into *S*-acetyl protection groups was performed according to an already described procedure using bromine in acetyl chloride and acetic acid.[45] By this method target compound **1** with *S*-acetyl-protected thiols on both ends was obtained as a yellowish solid in 96% yield after column chromatography. The synthesis of **5** is described in detail in ref 37. The terminally amino-functionalized biphenyl structure comprising two methyl groups in the 2,2′ positions **13** was assembled in a benzidine rearrangement reaction from 3-nitrotoluene following a literature procedure.[46] In a *Sandmayer*-type reaction, both amino groups of **13** have been substituted by iodines to afford **14** following a literature procedure.[47] In a one-pot reaction first both iodines were substituted by lithium atoms in a halogen−metal exchange reaction using *tert*-butyllithium in THF at −78 °C. Subsequent quenching with elemental sulfur followed by in situ protection with acetic anhydride in acetic acid afforded **5** as a white solid in 28% yield after column chromatography.

All compounds have been fully characterized by $^1H$ and $^{13}C$ NMR spectroscopy, mass spectroscopy, melting point, and elemental analysis. The target compounds **1**−**5** have been characterized further by UV−vis spectroscopy. In addition, the solid-state structure of **5** has been investigated by X-ray analysis.

**2.2. X-ray Analysis.** A single crystal of **5** was glued on a glass fiber using perfluoropolyether. Data were collected at 200 K on a STOE-IPDS2 diffractometer with graphite-monochromated Mo Kα radiation ($\lambda = 0.71073$ Å). The structures were solved by direct methods and refined by full-matrix least-squares analysis. **5**: $[C_{18}H_{18}O_2S_2]$; $M = 330.44$, orthorhombic, space group *Pbca*, $a = 18.257(4)$ Å, $b = 9.826(2)$ Å, $c = 18.866(4)$ Å, $\alpha = \beta = \gamma = 90°$, $V = 3384.4(12)$ Å$^3$, $Z = 8$, $D_c = 1.297$ g/cm$^3$, $\mu = 0.318$ mm$^{-1}$; 10 686 reflections measured, 3254 independent reflections, $R_{int} = 0.0531$, 2405 independent reflections with $F_o > 4\sigma(F_o)$; 199 parameters (S, O, C refined anisotropically, H atoms calculated at ideal positions), R1 = 0.0490, wR2 = 0.1588(all data), residual electron density 0.509 e/Å$^3$. Supplementary crystallographic data for **5** can be found in CCDC 286406.[48]

**2.3. Fabrication of SAMs.** The gold and silver substrates were prepared by thermal evaporation of 200 nm of gold or 100 nm of silver (99.99% purity) onto mica or polished single-crystal silicon (100) wafers (Silicon Sense) primed with a 5 nm titanium adhesion layer. The mica substrates were prelimi-

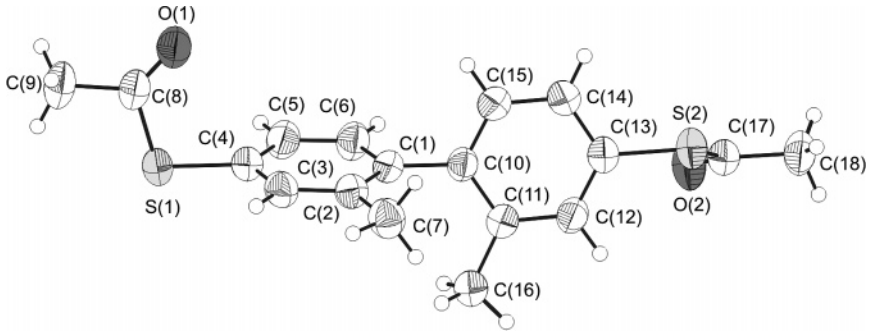


**Figure 2.** Solid-state structure of **5** (50% probability thermal ellipsoids). Selected bond lengths (pm) and angles (deg): S(1)−C(4) 177.6(3), S(1)−C(8) 178.2(3), O(1)−C(8) 120.1(4), C(1)−C(10) 148.7(3); C(4)−S(1)−C(8) 101.80(12), O(1)−C(8)−C(9) 124.4(3), O(1)−C(8)−S(1) 122.9-(2), C(9)−C(8)−S(1) 112.6(2).

nary annealed at 320 °C for 24 h prior to metal evaporation, done at the same temperature. The evaporated films were polycrystalline with a grain size of 20−50 nm for Si or a terrace size of 100−200 nm for mica as observed by atomic force microscopy and scanning tunneling microscopy. Both grains and terraces predominantly exhibit an (111) orientation.[49,50] SAMs **1**−**5** were formed by immersion of freshly prepared substrates into a 1 mmol solution of the respective substance in DMF at room temperature for 24 h. To remove the protection acetyl groups, an appropriate amount of either $NH_4OH$ or triethylamine (TEA) and water was added to the solution. After immersion, the SAM samples were carefully rinsed with the solvent, blown dry with argon, and kept, if necessary, for several days in argon-filled glass containers until characterization.

For some experiments, we used SAMs formed from biphenyl thiols (BPT, $C_6H_5$–$C_6H_4$–SH) as a direct reference to the BDDT films. The thiol group of the BPT molecule was not protected. The BPT SAMs were prepared on the same substrates and using the same fabrication procedure as the BDDT films but without addition of $NH_4OH$ or TEA to BPT solution.

**2.4. UV−vis Measurements.** For the UV−vis measurements, $1 \times 10^{-5}$ M solutions of compounds **1**−**5** in hexane were prepared. UV−vis spectra were recorded with a Varian Cary 500Scan UV−Vis−NIR spectrophotometer using 1 cm cuvettes. The measurements were performed at room temperature.

**2.5. HRXPS and NEXAFS Measurements.** The fabricated films were characterized by synchrotron-based HRXPS and angle-resolved NEXAFS spectroscopy. The measurements were carried out under UHV conditions at a base pressure better than $1.5 \times 10^{-9}$ mbar. All experiments were performed at room temperature. The spectra acquisition time was selected in such a way that no noticeable damage by the primary X-rays occurred during the measurements.[51−54]

The HRXPS experiments were performed at the bending magnet beamline D1011 at the MAX II storage ring of the MAX-lab synchrotron radiation facility in Lund, Sweden. For these measurements, only the films on mica were used. The C 1s and S 2p HRXPS spectra were collected in normal emission geometry at photon energies (PEs) of 350 and 580 eV. In addition, Au 4f and Ag 3d spectra were acquired and the O 1s range was monitored. The binding energy (BE) scale of every spectrum was individually calibrated using the Au $4f_{7/2}$ emission line of an Au substrate covered by an alkanethiolate SAM at 83.95 eV. The latter value is given by the latest ISO standard.[55] It is very close to a value of 83.93 eV, which has been obtained by us for Au $4f_{7/2}$ using a separate calibration to the Fermi edge of a clean Pt foil.[50] The energy resolution was better than 100 meV, which is noticeably smaller than the full-widths at half-maximum (fwhm) of the photoemission peaks addressed in this study.

HRXPS spectra were fitted by symmetric Voigt functions and either a Shirley-type or linear background. To the S $2p_{3/2,1/2}$ doublets we used a pair of such peaks with the same fwhm, a branching ratio of 2 ($2p_{3/2}/2p_{1/2}$), and a spin−orbit splitting (verified by fit) of ≈1.18 eV ($2p_{3/2}/2p_{1/2}$).[56] The fits were performed self-consistently: the same peak parameters were used for identical spectral regions. The accuracy of the resulting BE/fwhm values is 0.02−0.03 eV.

The NEXAFS spectroscopy measurements were performed at the HE-SGM beamline of the synchrotron storage ring BESSY II in Berlin, Germany. For these measurements mostly the films on silicon were used. The spectra acquisition was carried out at the C K-edge in the partial electron yield mode with a retarding voltage of −150 V. Linear polarized synchrotron light with a polarization factor of ≈82% was used. The energy resolution was ≈0.40 eV. The incidence angle of the light was varied from 90° (***E*** vector in surface plane) to 20° (***E*** vector near surface normal) in steps of 10°−20° to monitor the orientational order in the SAMs.[57]

The raw NEXAFS spectra were normalized to the incident photon flux by division through a spectrum of a clean, freshly sputtered gold sample. In the case of Ag substrate, a spectrum of clean silver was subtracted from the raw spectrum of a SAM sample before normalization.[58,59] The energy scale was referenced to the pronounced $\pi^*$ resonance of highly oriented pyrolytic graphite at 285.38 eV.[60]

## 3. Results

**3.1. X-ray Analysis.** Single crystals suitable for X-ray analysis of **5** have been obtained by slow diffusion of hexane into a solution of **5** in diethyl ether. Compound **5** crystallizes in the orthorhombic space group *Pbca*. The asymmetric unit is defined by the formula $C_{18}H_{18}O_2S_2$; hence, it contains only one molecule. The unit cell consists of eight asymmetric units and, hence, contains eight molecules **5**. The solid-state structure of **5** is displayed in Figure 2. Both phenyl rings of the biphenyl structure are planar with the methyl group in position 2 in the plane of the respective ring. The phenyl rings are rotated with respect to each other by a torsion angle of 79.7(2)°. Hence, the overlap of both adjacent $\pi$ systems and, thus, their conjugation is minimal in the solid-state structure. Due to rotation of the phenyl rings, the molecular structure of **5** does not have a center of inversion.

The bond length between the two phenyl rings [C(1)−C(10)] is 148.7(3) pm, which is close to the length of the $C(sp^2)$−$C(sp^2)$ bond in unsubstituted biphenyl (148 pm).[61] The molecular axis of the molecule can be defined by the sulfur atoms S(1) and S(2) and the bond between both phenyl rings, that is C(1)−C(10). The length along this molecular axis is given by an

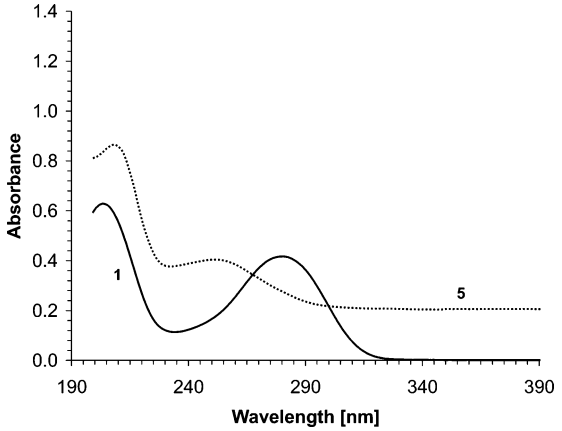


**Figure 3.** UV−vis spectra of compounds **1** (solid line) and **5** (dotted line). For better visibility the spectrum of **5** is shifted upward by 0.2 units.

intramolecular sulfur distance of 1.06(2) nm. The acetyl protection groups at the terminal sulfurs do not lie in the plane of the phenyl ring. The bond length between the sulfur and the aromatic carbon was determined to be 177.6(3) pm for S(1)−C(4) and 177.0(2) pm for S(2)−C(13), which lies between the usual lengths of C($sp^3$)−S (182 pm) and C($sp^2$)−S (175 pm) bonds.[61]

**3.2. UV−vis Spectroscopy.** Target compound **1** with the unsubstituted biphenyl backbone exhibits absorption maxima at 280.5 and 203.5 nm (see Figure 3), in good agreement with previous results (290 nm).[31] These maxima can be assigned to the benzene *p* and $\beta$ bands, respectively.[63] The *p* band levels off at about 325 nm. The shift of this band compared to the parent compound, biphenyl (247.7 nm), probably arises from the enlargement of the conjugated $\pi$ system due to substitution with lone pairs containing *S*-acetyl groups.[62] In contrast to **1**, the longest wavelength absorption of target compound **5** with two additional methyl groups in the 2 and 2′ positions is shifted hypsochromically to 251.5 nm. This maximum levels off at about 300 nm. A similar difference has been observed already between the spectra of biphenyl (247.7 nm) and 2,2′-dimethylbiphenyl (227 nm).[62,64] This blue shift of **5** compared to **1** indicates a lower $\pi$ conjugation of the substituted compound as a consequence of the increased torsion angle between both phenyl rings.

UV−vis spectra of target compounds **2**−**4** are presented in Figure 4. The absorption spectra of **2** and **3** look rather similar, in a like manner as for the parent compounds fluorene and 9,-10-dihydrophenanthrene.[62] In analogy to known compounds,[65] two observed absorptions of almost equal intensity at 311.5 and 290.0 nm for **2** can be assigned to the α and *p* bands, respectively, with the latter band being red shifted due to the presence of two *S*-acetyl groups extending $\pi$ conjugation. The broader more intense band at 211.5 nm corresponds to the $\beta$ band. The respective bands for **3** are observed at 312.5, 294.5, and 214.0 nm. The leveling off of the longest wavelength absorption occurs for both compounds at about 330 nm. The last member of this series **4** contains an ethenyl bridge between the 2 and 2′ positions, resulting in a phenanthrene $\pi$ system. Three absorption maxima are observed for this compound, namely, a broad maximum at 218.5 nm, the most intense maximum at 268.0 nm, and a weaker absorption at 292.5 nm, assigned to the $\beta$ band and *p* band (two latter maxima), respectively. In addition, the α band with a vibrational fine structure of five peaks between 326 and 359.0 nm was found.

Taking the leveling off of the longest wavelength absorption as an indicator for the degree of the $\pi$-system conjugation, we

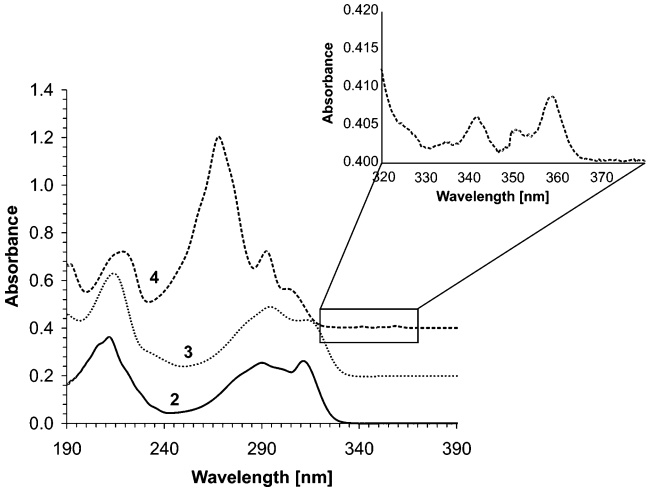


**Figure 4.** UV−vis spectra of compounds **2** (solid line), **3** (dotted line), and **4** (dashed line). For better visibility the spectra of **3** and **4** are shifted upward by 0.2 and 0.4 units, respectively.

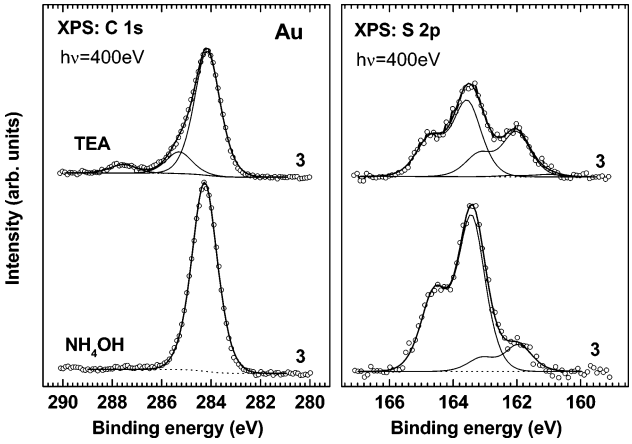


**Figure 5.** C 1s (left) and S 2p (right) HRXPS spectra of **3**/Au (open circles) prepared using deprotection by TEA (top) and $NH_4OH$ (bottom). The spectra are decomposed into individual contributions (thin solid lines). The overall fit curves are given by thick solid lines. Background is shown by dotted line.

can conclude that target compounds **1**−**3** with an absorption cutoff between 325 and 330 nm all have comparable degrees of $\pi$ conjugation. Considerably increased $\pi$ conjugation is observed for target compound **4** with absorptions that reach 370 nm. As **4** consists of a phenanthrene core with fully delocalized $\pi$ electrons, this increased conjugation is not surprising. As expected, reduced conjugation is observed in **5**, with the absorption cutoff at about 300 nm. Obviously the induced steric strain provided by the methyl groups in the ortho positions enlarges the torsion angle between both phenyl rings and, hence, reduces the overlap of both $\pi$ systems considerably.

**3.3. HRXPS.** C 1s and S 2p HRXPS spectra of **3**/Au prepared using a deprotection by TEA and $NH_4OH$ are presented in Figure 5. Similar spectra were observed for all BDDT SAMs of this study, so that the spectra in Figure 5 are representative for the entire series. The spectra are decomposed into individual contributions (thin solid lines) using a self-consisting fitting procedure and reasonable assumptions about the presence of definite chemical species in the investigated films. In the C 1s spectra for the $NH_4OH$-deprotected SAMs, a single emission at 284.2−284.3 eV is observed. This emission is assigned to the aromatic backbone of the BBDT SAMs. In the respective spectrum of the TEA deprotected SAMs, the emission at 284.2−284.3 eV is accompanied by a high BE shoulder at 285.2−

**TABLE 2: Average Peak Positions (eV) and fwhm (eV) for the TEA-Deprotected BDDT SAMs and BPT Films (as a reference). Data Were Derived from the HRXPS Spectra Acquired at a Photon Energy of 350 eV**

| | Au | | Ag | |
|---|---|---|---|---|
| | BE position | fwhm | BE position | fwhm |
| C1s main | 284.24 ± 0.08 | 1.06 ± 0.05 | 284.24 ± 0.10 | 1.00 ± 0.04 |
| C1s shoulder | 285.24 ± 0.08 | 1.05 ± 0.05 | 285.20 ± 0.07 | 1.08 ± 0.04 |
| C1s Cd0 | 287.63 ± 0.05 | 0.61 ± 0.05 | 287.58 ± 0.05 | 0.70 ± 0.05 |
| $S2p_{3/2}$ thiolate | 162.07 ± 0.03 | 0.63 ± 0.03 | 161.99 ± 0.03 | 0.53 ± 0.03 |
| $S2p_{3/2}$ thiol | 163.47 ± 0.03 | 0.76 ± 0.03 | 163.43 ± 0.03 | 0.73 ± 0.03 |
| C1s for BPT | 284.17 | 0.81 | 284.38 | 0.83 |
| $S2p_{3/2}$ for BPT | 162.04 | 0.64 | 162.10 | 0.57 |

285.3 eV and a low-intensity peak at 287.6 eV. The higher BE shoulder is typical of biphenyl-derived SAMs; it has been alternatively assigned to a shake-up excitation in the aromatic matrix and to the carbon atom bound to sulfur,[50,66−71] with the most recent experimental data favoring the latter assignment.[71] A low-intensity peak at 287.6 eV can be assigned to the acetyl protection groups, which were not removed by the deprotection procedure. We assume that all these groups are located at the SAM−ambient interface, whereas the second thiol group of the respective molecules is deprotected and makes a thiolate-type bonding to the substrate. The molecules with both thiol groups remaining protected will make only a weak bonding to the substrate and be substituted by the molecules, in which at least one of the thiol groups is deprotected. According to our estimates, about 10−20% of the thiol tail groups in the TEA-deprotected SAMs keep their protection group.

In the S 2p spectra of the BBDT SAMs, two S $2p_{3/2,1/2}$ doublets with S $2p_{3/2}$ at 162.0 and 163.4−163.5 eV are observed. These doublets can be clearly assigned to the thiolate-type sulfur bound to the metal surface[50,72] and to the thiol tail group,[39,53] respectively. The intensity of the thiolate component is noticeably lower than that of the thiol one, which is understandable considering the attenuation of the thiolate signal by the hydrocarbon overlayer.

The average peak positions and fwhm of the individual emissions for the TEA-deprotected BDDT SAMs and BPT films (as a reference) are compiled in Table 2. The assignments of these emissions are supported by their intensity changes with varying probing depth of the photoelectrons. This is illustrated by Figure 6, where the C 1s and S 2p HRXPS spectra of the TEA-deprotected **1**/Ag acquired at PEs of 350 and 580 eV are presented. With increasing kinetic energy of the photoelectrons (i.e., going from a PE of 350 to 580 eV, the relative spectral weights of the acetyl-assigned peak in the C 1s spectra and thiol-assigned peak in the S 2p spectra decrease, as can be expected for moieties located at the SAM−ambient interface.

The $NH_4OH$-deprotected films exhibit much higher total C1s intensity than the TEA-deprotected ones. In accordance with this observation, the effective film thicknesses of the former SAMs are much larger than those of the latter ones (see Tables 3 and 4). Note that the thickness values were calculated according to a standard procedure[74] using the intensity ratios of the C1s and Au4f/Ag3d signals and standard attenuation lengths for the Au 4f, Ag 3d, and C 1s emissions;[75] the accuracy of the thickness values is ±5%. Comparison of the effective thicknesses with the molecular lengths of the targets **1**−**5** (about 15 Å) suggests formation of a monolayer with inclined SAM constituents in the case of TEA deprotection and building of a multilayer in the case of $NH_4OH$ deprotection. These results are supported by analysis of the S 2p spectra (see, e.g., Figure 5). If corrected for signal attenuation, the intensity ratios of the thiol and thiolate components for the TEA-deprotected BDDT SAMs are close to 1:1, as should be for a monolayer, whereas the 1:1 ratio cannot be reproduced for the $NH_4OH$-deprotected films.

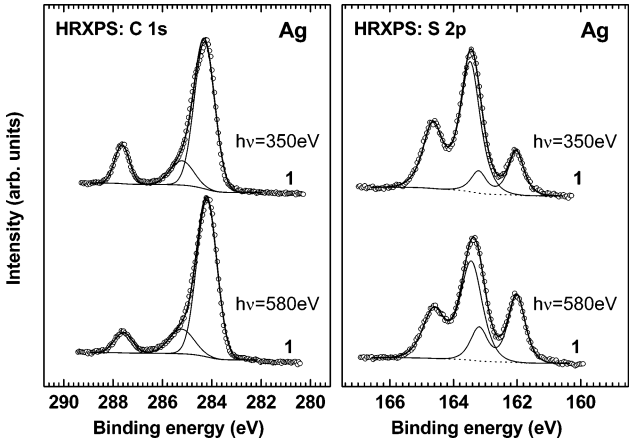


**Figure 6.** C 1s (left) and S 2p (right) HRXPS spectra of **1**/Ag (deprotection by TEA) acquired at PEs of 350 and 580 eV. The spectra are decomposed into individual contributions (thin solid lines). The overall fit curves are given by thick solid lines. Background is shown by dotted line.

**TABLE 3: Effective Film Thickness (Å) and Average Tilt Angle (deg) of the Aromatic Backbones in SAMs 1−5 Prepared Using Deprotection by TEA. For Comparison, Values for the BPT SAMs Are Given (length of the BPT molecules is 10.25 Å, and the substrate−S distance was estimated to be 2.4 Å,[73] which gives 12.65 Å as the ultimate thickness of the BPT SAM)**

| | Au | | Ag | |
|---|---|---|---|---|
| SAM | thickness | tilt angle | thickness | tilt angle |
| 1 | 12.7 | 33.3 | 13.7 | 21.1 |
| 2 | 12.1 | 33.8 | 13.8 | 23.0 |
| 3 | 11.9 | 38.2 | 13.6 | 24.0 |
| 4 | 12.2 | 34.7 | 14.3 | 20.3 |
| 5 | 10.2 | 39.5 | 12.5 | 26.0 |
| BPT | 11.6 | 23.0 | 12.1 | 18.0 |

**TABLE 4: Effective Film Thickness (Å) and Average Tilt Angle (deg) of the Aromatic Backbones in SAMs 1−5 Prepared Using Deprotection by $NH_4OH$. For Comparison, the Values for the BPT SAMs Are Given**

| | Au | | Ag | |
|---|---|---|---|---|
| SAM | thickness | tilt angle | thickness | tilt angle |
| 1 | 19.9 | 33.4 | 24.5 | 38.1 |
| 2 | 15.3 | 36.0 | 21.7 | 37.9 |
| 3 | 16.9 | 39.3 | 24.5 | 39.8 |
| 4 | 17.4 | 38.4 | 23.8 | 39.2 |
| 5 | 18.3 | 36.0 | 19.1 | 38.6 |
| BPT | 11.6 | 23.0 | 12.1 | 18.0 |

According to Tables 3 and 4, the films on Ag are generally thicker than those on Au, which suggests a smaller molecular inclination in the former SAMs. A comparison between the HRXPS spectra of the BDDT SAMs on Au and Ag is given by Figure 7, where the C1s and S2p HRXPS spectra for **4**/Au and **4**/Ag (TEA deprotection) are presented. In these spectra the features related the SAM−ambient interface (the "acetyl" in the C1s spectra and the "thiol" in the S 2p spectra) have a larger intensity for Ag than for Au. These intensity relations imply that the films on Ag are thicker than those on Au, in accordance with the previous statement on the basis of the thickness values.

**3.4. NEXAFS Spectroscopy.** C K-edge NEXAFS spectra of **3**/Ag prepared using deprotection by TEA and $NH_4OH$ are presented in Figure 8. The spectra in the left panel were acquired at the magic angle of X-ray incidence (the spectrum is

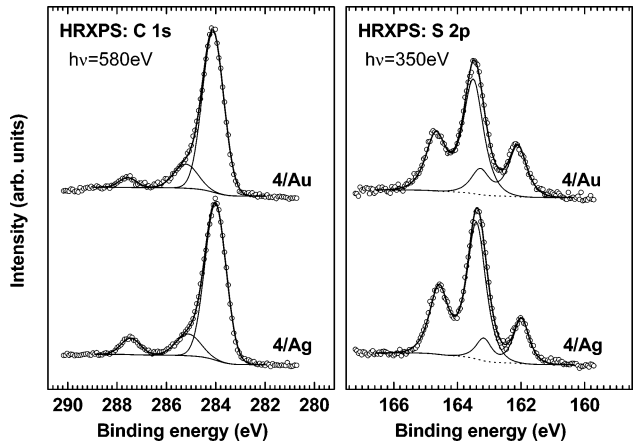


**Figure 7.** C 1s (left) and S 2p (right) HRXPS spectra of **4**/Au and **4**/Ag (deprotection by TEA) acquired at PEs of 580 (C 1s) and 350 eV (S 2p). The spectra are decomposed into individual contributions (thin solid line). The overall fit curve is given by a thick solid line. Background is shown by dotted line.

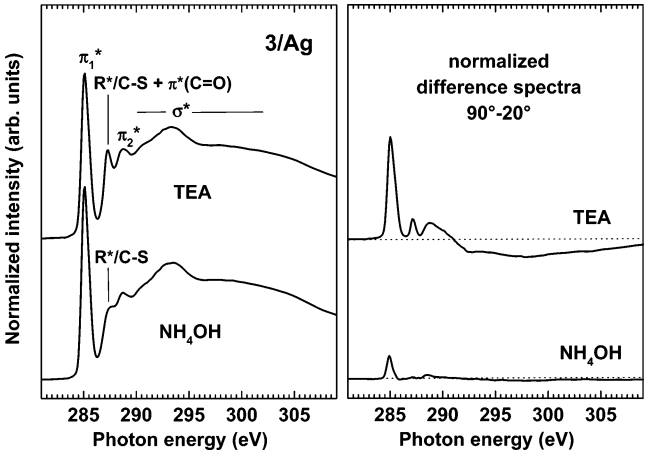


**Figure 8.** C K-edge NEXAFS spectra of **3**/Ag (deprotection by TEA and $NH_4OH$) acquired at an X-ray incidence angle of 55° (left) and the difference between the spectra acquired at X-ray incidence angles of 90° and 20° (right). The characteristic absorption resonances are marked.

independent of the molecular orientation),[57] while the curves in the right panel are the difference between the spectra acquired at X-ray incidence angles of 90° and 20°. Similar spectra and difference curves were observed for all BDDT SAMs of this study (see below for details), so that the data in Figure 8 are to a definite extent representative for the entire series. The spectra are dominated by the intense $\pi_1$* resonance of the phenyl rings at ≈285.1 eV, which is accompanied by the respective $\pi_2$* resonance at 288.8 eV, the R*/C−S* resonance at ≈287.8 eV, and several broad $\sigma$* resonances at higher photon energies (the assignment has been performed in accordance with refs 26, 38, 76, and 77).

The R*/C−S* resonance is much stronger in the TEA case as compared to the $NH_4OH$ deprotection. Taking into account the HRXPS data, it can be explained assuming that this resonance overlaps with the $\pi$*(C═O) resonance (286.0−288.5 eV)[57,78] of the residual acetyl groups in the TEA case. Also, in accordance with the HRXPS results, the difference spectrum of the TEA-deprotected SAMs exhibit pronounced linear dichroism characteristic of a well-ordered SAM, whereas only a very small dichroism is observed in the $NH_4OH$ case, which can be expected for a disordered multilayer film. Note that the sign of the difference peaks in the difference spectra of the TEA-deprotected SAMs suggests an upright orientation of the biphenyl backbones in these films.

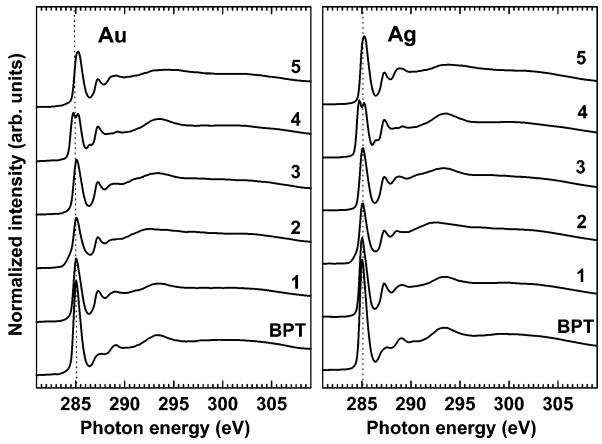


**Figure 9.** C K-edge NEXAFS spectra of the TEA-deprotected SAMs **1**−**5** on Au (left) and Ag (right) acquired at an X-ray incidence angle of 55°.

Apart from the above qualitative consideration, the spectra of the different SAMs were considered in detail and a quantitative evaluation of the NEXAFS data was performed. The C K-edge NEXAFS spectra of the TEA-deprotected SAMs **1**−**5** and BPT SAMs on Au and Ag acquired at an X-ray incidence angle of 55° are presented in Figure 9. It is clearly seen that the spectra of the individual SAMs do not exhibit any noticeable differences for Au and Ag and that the pattern of the absorption resonances in all the SAMs except **4** is quite similar, as described above. The higher intensity of the R*/C−S* resonance in SAMs **1**−**5** as compared to the BPT film is related to the additional contribution of the $\pi$*(C═O) resonance. The pattern of the absorption resonances for SAMs **1**−**3** and **5** (and for the BPT SAMs as well) is very similar to those of benzene,[79−81] which, in the case of **1**, is related to localization of the excited molecular orbitals by creation of a C1s core hole.[80] This localization can be associated with a rather low degree of conjugation between the individual rings comprising the biphenyl moiety in the respective molecule. Obviously, even the introduction of the aliphatic bridge between the phenyl rings as it happens in **2** and **3** does not result in a noticeable improvement of the conjugation along the biphenyl backbones in the respective SAMs. At the same time, the ring conjugation in SAM **5** is comparably smaller, as can be observed by closer inspection of the energies of the $\pi_1$* resonance. In fact, while the energy positions of the $\pi_1$* resonance for the BPT films and SAMs **1**−**3** practically coincide (285.1 eV), this position is slightly higher for SAMs **5** (285.2 eV). The latter value coincides with the analogous value for benzene in the gas state,[79] which can be considered as indirect evidence that the individual rings in the SAM constituents of film **5** have a lower degree of conjugation (or no conjugation at all) than those in SAMs **1**−**3**.

At the same time, a different situation occurs for SAM **4**, for which the splitting of the $\pi_1$* resonance to two peaks at 284.8 and 285.2 eV and the appearance of an additional weak $\pi_1$* resonance at 286.4 eV are observed. Such splitting of the $\pi_1$* resonance is characteristic of conjugated aromatic systems.[82] In particular, it was observed in the NEXAFS spectra of solid tetracene and pentacene[80] and anthracenethiolate SAMs.[26] In the latter case, the splitting was related to the chemical shift of the two symmetry-independent carbon atoms of anthracenethiolate with strong influence of excitonic effects.[26,80] The appearance of an additional weak resonance at 286.4 eV can be related to the further splitting of the $\pi$* resonance pattern

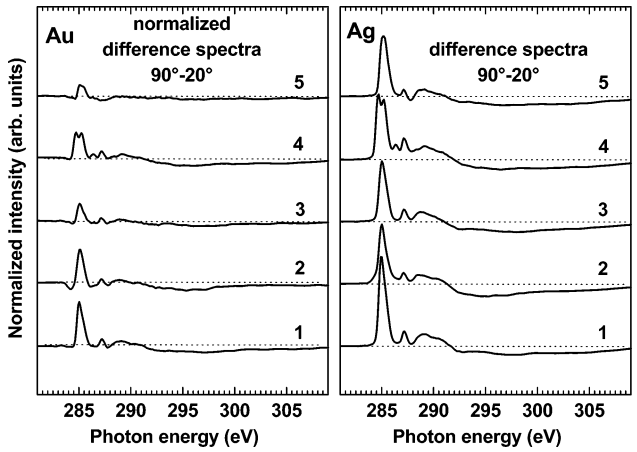


**Figure 10.** C K-edge NEXAFS difference (90°−20°) spectra of the TEA-deprotected SAMs **1**−**5** on Au (left) and Ag (right).

stemming from the nonequivalency of the individual carbon atoms in molecule **4**.[57]

Generally, if the assignment of the high-BE shoulder in the C1s HRXPS spectra to the carbon atom bound to sulfur is correct, one has to expect the appearance of the additional, even though low intensity, $\pi_1$* resonance in the C K-edge NEXAFS spectra of all BDDT SAMs.[57] Such a resonance is not observed. However, the $\pi_1$* resonance in BDDT SAMs is noticeably broader and more asymmetric that the respective resonance of the BPT film, which can be related to the presence of an additional feature at the high-PE side of the main peak. This feature can be tentatively associated with the additional $\pi_1$* resonance related to the carbon atoms bound to sulfur.

Along the differences in the pattern of the absorption resonances, BDDT SAMs exhibit differences in the average inclination of the SAM constituents and degree of molecular orientation. These differences are highlighted by the C K-edge NEXAFS difference spectra of the TEA-deprotected SAMs **1**−**5** on Au and Ag presented in Figure 10. The spectra exhibit much larger linear dichroism in the case of Ag, which suggests that the average molecular inclination in the BDDT SAM on Ag is much smaller than that in the films on Au. Also, there are pronounced differences in the linear dichroism between the individual SAMs on both Au and Ag.

Apart from these conclusions, average tilt angles of the biphenyl backbone in the BDDT SAMs were derived by a standard numerical evaluation of the NEXAFS data.[57] In particular, for a vector-type orbital, the intensity of an absorption resonance $I$ is given by[57]

$$I(\alpha,\theta) = A\left\{P \times \left(\frac{1}{3}\right)\left[1 + \frac{1}{2}\cdot(3\cos^2\theta - 1)(3\cos^2\alpha - 1)\right] + (1-P)\frac{1}{2}\sin^2\alpha\right\} \quad (1)$$

where $A$ is a constant, $P$ is a polarization factor of the X-rays, $\theta$ is the X-ray incidence angle, and $\alpha$ is the average tilt angle of the molecular orbital.[57] This formula was slightly modified for the case of aromatic SAMs, taking into account that the orientation of the backbone is given not by one but two angles: the tilt angle $\varphi$ of the backbone axis with respect to the surface normal and the twist angle $\vartheta$ of the aromatic rings with respect to the plane spanned by the surface normal and the molecular axis. Selecting the most prominent $\pi_1$* resonance of the aromatic backbone for the evaluation procedure, one can take use of the following relation between the tilt angle $\alpha$ of the $\pi_1$* orbital and the angles $\varphi$ and $\vartheta$[26,83]

$$\cos\alpha = \cos\vartheta \sin\varphi \quad (2)$$

Introducing this relation into expression 1, one can determine the average tilt angles of the biphenyl backbones in the BDDT SAMs from the NEXAFS data as long as the twist angles of these backbones are known. Considering the structure of the BDDT molecules in the respective SAMs, it is reasonable to assume their herringbone arrangement, which is characteristic of aromatic bulk systems[32,84−86] and is believed to be the case for aromatic SAMs as well.[25,83,87,88] Within this most probable structure, two different spatial orientations of aromatic moieties occur with reverse twist angles $\vartheta_1 = -\vartheta_2$ and the same tilt angles $\varphi_1 = \varphi_2$, with the sign of the twist angle of no importance since cos $\vartheta$ is an even function. The most reasonable assumption for the absolute value of the twist angle is 32° as found for both aromatic bulk systems[32,84−86] and SAM-like films.[87,88] Note that we assume the coplanar arrangement of the individual rings within the biphenyl backbone, which is true for the molecules **1**, **2**, and **4**, an approximation for molecule **3**, and a simplification for molecule **5** (see Table 1).

The derived average tilt angles of the biphenyl backbones in the BDDT SAMs are compiled in Tables 3 and 4 for the TEA- and $NH_4OH$-deprotected films, respectively. The accuracy of the fits according to eq 1 is ±0.5°, but the general accuracy of the derived values can be somewhat higher in view of the upper estimate for the accuracy of the NEXAFS experiments (±5°) and the uncertainty of the twist angles. Note that the tilt angles in Tables 3 and 4 represent average values over the macroscopic area of the films and are a fingerprint of the orientational order. According to Table 4, the molecular inclination is the latter films is quite large on both Au and Ag, which is understandable considering that these films are multilayers. In contrast, the average tilt angles of the TEA-deprotected SAMs exhibit a strong substrate effect (see Table 3) with noticeably smaller values for Ag as compared to Au. At the same time, for both Au and Ag the average tilt angles of the BDDT SAMs are much larger than the respective values for the nonsubstituted biphenyl SAMs, which clearly shows the effect of the thiol tail group at the 4′ position. Comparing the average tilt angles for the different BDDT SAMs on the same substrate to each other, we do not see pronounced differences except, probably, slightly and noticeably higher values for SAMs **3** and **5**, respectively. Considering that the molecular constituents of both films do not have a planar conformation in the solid phase (see Table 1), this result suggests that a nonzero torsion between the individual rings of the biphenyl backbone hinders an effective packing of the BDDT molecules. At the same time, introduction of the aliphatic bridge between the individual phenyl rings (as in molecules **2** and **4**) does not have any noticeable effect on the molecular structure of the respective SAMs.

Looking at the results in a different way, one can state that similar values of the average tilt angles for SAMs **1**, **2**, and **4** and the distinct difference of these values from the analogous values for SAMs **3** and **5** suggest that SAMs **1**, **2**, and **4** are characterized by a similar molecular conformation of the SAM constituents, which is distinctly different from that in SAMs **3** and **5**. Since the constituents of SAMs **2** and **4** definitely have a planar conformation, the same conformation can be assumed for the constituents of SAMs **1**, removing the last controversy, which still exists despite the crystallographic data for the respective parent compound in the solid state.[32,33]

## 4. Discussion

The conjugation along the biphenyl backbone in the series of model compounds **1**−**5** has been investigated in solution by

UV−vis spectroscopy and in the SAMs by NEXAFS spectroscopy. According to both experiments, compound **4** containing a fully delocalized phenanthrene $\pi$ system displays the highest extent of delocalization within the series. On the other end, target compound **5** with a large intramolecular torsion angle in both the molecular and the solid state displays the lowest degree of conjugation.

The HRXPS and NEXAFS data on the BDDT SAMs are in good agreement with each other. An important result is a strong dependence of the film quality on the deprotection procedure. Whereas densely packed SAMs were formed in the case of TEA deprotection, bilayer or multilayer films were prepared as long as $NH_4OH$ was used as the deprotection agent. Interestingly, not all but 80−90% of the thiol tail groups were deprotected in the TEA case, so that the SAM−ambient interface was comprised of both acetyl-protected (10−20%) and deprotected (80−90%) thiol moieties. In the $NH_4OH$ case, all thiol moieties were deprotected; there was no trace of acetyl in the resulting multilayer film. Probably, the residual protected tail groups represent a stabilizing factor for the SAM formation.

Anyway, to form molecular monolayers, TEA seems to be a favorable deprotection agent compared with $NH_4OH$, which is usually used for deprotection of acetyl-protected aromatic dithiols.[30,31] However, limited data sets of the previous publication[30,31] do not allow unequivocal conclusions on the quality of the respective SAMs (SAMs **1** and **2** on Au—only these two SAMs have been studied previously), even though the authors of refs 30 and 31 claimed that SAM-like films were formed. It was also stated that the self-assembly of conjugated mono- or dithiols has to be performed in a dilute solution ($\ll$1 mM) to avoid multilayer formation.[31] However, no evidence for this statement has been provided.

Note that the biphenyl-based dithiol SAMs can also be prepared from the nonprotected target compounds,[27,30,31] even though the most detailed spectroscopic study claims that organodithiols with a short oligophenyl backbone, such as phenyl or biphenyl, do not form well-oriented SAM-like films but a multilayer consisting of oligomers of the dithiol molecules.[38]

Comparison of the BDDT SAMs with the films formed from the respective nonsubstituted biphenylthiols (BPT) suggests that introduction of the thiol group at the 4′ position of the biphenyl backbone complicates the formation of a densely packed and well-ordered SAM on both Au and Ag. This effect is especially pronounced in the case of the Au substrate, where a low orientational order and a large molecular inclination are observed in the BDDT SAMs. In contrast, the BDDT films on Ag exhibit a much higher quality, which is only slightly inferior to that of BPT/Ag. A comparable quality in the case of the Au substrate can only be achieved by introduction of methylene linkages between the thiol groups and biphenyl moiety.[39]

Comparing the different BDDT SAMs on the same substrate to each other, we can conclude that introduction of a side bridge between the individual rings of the biphenyl moiety does not affect the structure and quality of the respective SAMs to a noticeable extent as long as the molecule has a planar conformation in the densely packed films. Deviation from the planar conformation leads to the deterioration of the SAM quality and decreasing orientational order. It is evidenced by the example of SAM **3** and, especially, SAM **5**, where rather bulky methyl moieties were attached to the biphenyl backbone of the target molecule, ensuring a considerable torsion angle in solution as well as in the solid state. Presumably, the relative rotation of the individual rings makes it difficult to achieve an optimal $\pi-\sigma$ interaction, responsible for the molecular packing between the neighbor molecules in the SAM. We believe that the minimization of the respective energy contribution is exactly the reason for the change of the molecular conformation from nonplanar (gas phase) to planar in the solid phase. Of course, such a change is not always possible, as it, e.g., is the case for the compounds **3** and **5**.

Interestingly, the structure and quality of SAM **4** comprised of strongly conjugated molecules were comparable to these of SAM **1**, where a simple biphenyl spacer was used. This finding agrees with the results of the previous study[26] in which, by the example of SAMs formed from BPT and anthracenethiols on Au and Ag, it was shown that higher molecular conjugation and rigidity of the molecular backbone have only a slight effect on the final molecular orientation within the respective SAMs.

## 5. Conclusions

Acetyl-protected biphenyl-based dithiol derivatives (**1**−**5**) with different aliphatic substituents in the 2 and 2′ positions were synthesized and fully characterized. The substitution included introduction of an aliphatic bridge between the individual rings or attachment of bulky side groups, which made it possible to control the conformation of the biphenyl backbone. In particular, the torsion angle between both phenyl rings has been set and therewith the degree of intramolecular conjugation has been imposed in the molecular and solid state. The target BDDT compounds were used to fabricate SAMs on the evaporated Au(111) and Ag(111) substrates. Deprotection of the molecules was performed in situ during the SAM preparation, adding either $NH_4OH$ or TEA to the respective solution of acetyl-protected biphenyl derivatives. The fabricated BDDT films were characterized by HRXPS and NEXAFS spectroscopy. Whereas deprotection by $NH_4OH$ resulted in formation of multilayer films, deprotection by TEA allowed the preparation of densely packed BDDT SAMs. In the latter SAMs not all protection groups were removed, so that the SAM−ambient interface was comprised of 80−90% of the thiol group and 10−20% of the acetyl-protected ones.

The BDDT SAMs on Au exhibited a low orientational order and a large inclination of the SAM constituents. In contrast, a high orientational order and small molecular inclination, comparable to that in the nonsubstituted biphenyl SAMs, was found in the BDDT SAMs on Ag. Introduction of the alkyl bridge between the individual rings of the biphenyl backbone, resulting in its larger rigidity and a higher degree of intermolecular conjugation, did not lead to a noticeable change in the structure and packing density of the BDDT SAMs as long as the molecule has a planar conformation in the densely packed films. Deviation from the planar conformation resulted in deterioration of the film quality and a decrease of the orientational order, which was especially pronounced in the case of the large dihedral angle (SAM **5**).

Comparison of the experimental data for the nonsubstituted (**1**) and 2/2′-substituted (**2**−**4**) BDDT SAMs suggests a planar conformation of the molecular constituents in oligophenyl-derived SAMs on noble-metal substrates, in accordance with the crystallographic data for the respective parent compounds in the solid state.[32,33]

**Acknowledgment.** We thank M. Grunze for support of this work, A. Küller for providing us with the BPT substance, Ch. Wöll (Universität Bochum) for providing us with the equipment for the NEXAFS measurements, E. Moons, S. Watcharinyanon, and L. S. O. Johansson (Karlstad University) for cooperation

at MAX-lab, and the BESSY II and MAX-lab staff for assistance during the experiments at the synchrotrons. This work was supported by the German BMBF (05KS4VHA/4 and 05 ES3XBA/5) and European Community (Access to Research Infrastructure action of the Improving Human Potential Programme).

**Supporting Information Available:** Complete synthetic protocols of all described compounds together with their spectroscopic data as well as crystallographic data for **5**. This material is available free of charge via the Internet at http://pubs.acs.org.

## References and Notes

(1) *International Roadmap for Semiconductors*; 2003.
(2) Kuhn, H.; Möbius, D. *Angew. Chem.* **1971**, *83*, 672−676; *Angew. Chem., Int. Ed. Engl.* **1971**, *10*, 460.
(3) Aviram, A.; Ratner, M. A. *Chem. Phys. Lett.* **1974**, *29*, 277.
(4) Mayor, M.; Weber, H. B.; Waser, R. In *Nanoelectronics and Information Technology*; Waser, R., Ed.; Wiley-VCH: Weinheim, 2003; p 501.
(5) Wassel, R. A.; Gorman, C. B. *Angew. Chem* **2004**, *116*, 5230−5233; *Angew. Chem., Int. Ed.* **2004**, *43*, 5120.
(6) Kagan, C. R.; Ratner, M. A. *MRS Bull.* **2004**, *29*, 376.
(7) James, D. K.; Tour, J. M. *Chem. Mater.* **2004**, *16*, 4423.
(8) McCreery, R. L. *Chem. Mater.* **2004**, *16*, 4477.
(9) Kushmerick, J. G.; Holt, D. B.; Pollack, S. K.; Ratner, M. A.; Yang, J. C.; Schull, T. L.; Naciri, J.; Moore, M. H.; Shashidhar, R. *J. Am. Chem. Soc.* **2002**, *124*, 10654.
(10) Holmlin, R. E.; Ismagilov, R. F.; Haag, R.; Mujica, V.; Ratner, M. A.; Rampi, M. A.; Whitesides, G. M. *Angew. Chem.* **2001**, *113*, 2378−2382; *Angew. Chem., Int. Ed.* **2001**, *40*, 2316.
(11) Cui, X. D.; Primak, A.; Zarate, X.; Tomfohr, J.; Sankey, O. F.; Moore, A. L.; Moore, T. A.; Gust, D.; Harris, G.; Lindsay, S. M. *Science* **2001**, *294*, 571.
(12) Xu, B.; Tao, N. J. *Science* **2003**, *301*, 1221.
(13) Reichert, J.; Ochs, R.; Beckmann, D.; Weber, H. B.; Mayor, M.; v. Löhneysen, H. *Phys. Rev. Lett.* **2002**, *88*, 176804/1.
(14) Elbing, M.; Ochs, R.; Koentopp, M.; Fischer, M.; von Hänisch, C.; Weigend, F.; Evers, F.; Weber, H. B.; Mayor, M. *Proc. Natl. Acad. Sci. U.S.A.* **2005**, *102*, 8815.
(15) Mayor, M.; v. Hänisch, C.; Weber, H. B.; Reichert, J.; Beckmann, D. *Angew. Chem.* **2002**, *114*, 1228−1231; *Angew. Chem., Int. Ed.* **2002**, *41*, 1183.
(16) Schull, T. L.; Kushmerick, J. G.; Patterson, C. H.; George, C.; Moore, M. H.; Pollack, S. K.; Shashidhar, R. *J. Am. Chem. Soc.* **2003**, *125*, 3202.
(17) Mayor, M.; Weber, H. B.; Reichert, J.; Elbing, M.; v. Hänisch, C.; Beckmann, D.; Fischer, M. *Angew. Chem.* **2003**, *115*, 6014−6018; *Angew. Chem., Int. Ed.* **2003**, *42*, 5834.
(18) Weber, H. B.; Reichert, J.; Weigend, F.; Ochs, R.; Beckmann, D.; Mayor, M.; Ahlrichs, R.; v. Löhneysen, H. *Chem. Phys.* **2002**, *281*, 113.
(19) Patrone, L.; Palacin, S.; Bourgoin, J. P. *Appl. Surf. Sci.* **2003**, *212−213*, 446.
(20) Love, J. C.; Estroff, L. A.; Kriebel, J. K.; Nuzzo, R. G.; Whitesides, G. M. *Chem. Rev.* **2005**, *105*, 1103.
(21) Ulman, A. *An Introduction to Ultrathin Organic Films: Langmuir−Blodgett to Self-Assembly*; Academic Press: New York, 1991; *Chem. Rev.* **1996**, *96*, 1533.
(22) *Thin films: self-assembled monolayers of thiols*; Ulman, A., Ed.; Academic Press: San Diego, CA, 1998.
(23) Schreiber, F. *Prog. Surf. Sci.* **2000**, *65*, 151.
(24) Sabatani, E.; Cohen-Boulakia, J.; Bruening, M.; Rubinstein, I. *Langmuir* **1993**, *9*, 2974.
(25) Himmel, H.-J.; Terfort, A.; Wöll, Ch. *J. Am. Chem. Soc.* **1998**, *120*, 12069.
(26) Frey, S.; Stadler, V.; Heister, K.; Eck, W.; Zharnikov, M.; Grunze, M.; Zeysing, B.; Terfort, A. *Langmuir* **2001**, *17*, 2408.
(27) Kang, J. F.; Ulman, A.; Liao, S.; Jordan, R.; Yang, G. H.; Liu, G.-Y. *Langmuir* **2001**, *17*, 95.
(28) Ulman, A. *Acc. Chem. Res.* **2001**, *34*, 855.
(29) Stapleton, J. J.; Harder, P.; Daniel, T. A.; Reinard, M. D.; Yao, Y.; Price, D. W.; Tour, J. M.; Allara, D. L. *Langmuir* **2003**, *19*, 8245.
(30) Tour, J. M.; Jones, L., II; Pearson, D. L.; Lamba, J. S.; Burgin, T. P.; Whitesides, G. M.; Allara, D. L.; Parikh, A. N.; Atre, S. V. *J. Am. Chem. Soc.* **1995**, *117*, 9529.
(31) de Boer, B.; Meng, H.; Perepichka, D. F.; Zheng, J.; Frank, M. M.; Chabal, Y. J.; Bao, Z. *Langmuir* **2003**, *19*, 4272.
(32) Trotter, J. *Acta Crystallogr.* **1961**, *14*, 1135.
(33) Hargreaves, A.; Rizvi, S. H. *Acta Crystallogr.* **1962**, *15*, 365.
(34) Brown, G. M.; Bortner, M. H. *Acta Crystallogr.* **1954**, *7*, 139.
(35) Cosmo, R.; Hambley, T. W.; Sternhell, S. *J. Org. Chem.* **1987**, *52*, 3119.
(36) Trotter, J. *Acta Crystallogr.* **1963**, *16*, 605.
(37) Elbing, M. Ph.D. Thesis, University of Karlsruhe and Forschungszentrum Karlsruhe GmbH, Karlsruhe, Germany, 2004.
(38) Azzam, W.; Wehner, B. I.; Fisher, R. A.; Terfort, A.; Wöll, Ch. *Langmuir* **2002**, *18*, 7766.
(39) Tai, Y.; Shaporenko, A.; Rong, H.-T.; Buck, M.; Eck, W.; Grunze, M.; Zharnikov, M. *J. Phys. Chem. B* **2004**, *108*, 16806.
(40) Becker, H. G. O.; et al. *Organikum*; Wiley-VCH: Weinheim, 2001.
(41) Cogolli, P.; Testaferri, L.; Tingoli, M.; Tiecco, M. *J. Org. Chem.* **1979**, *44*, 2636.
(42) Testaferri, L.; Tiecco, M.; Tingoli, M. *J. Org. Chem.* **1980**, *45*, 4376.
(43) Oh, H. K.; Woo, S. Y.; Shin, C. H.; Park, Y. S.; Lee, I. *J. Org. Chem.* **1997**, *62*, 5780.
(44) Wirth, H. O.; Gönner, K. H.; Kern, W. *Makromol. Chem.* **1963**, *63*, 53.
(45) Blaszczyk, A.; Elbing, M.; Mayor, M. *Org. Biomol. Chem.* **2004**, *2*, 2722.
(46) Wenner, W. *J. Org. Chem.* **1952**, *17*, 523.
(47) Fuji, K.; Yamada, T.; Fujita, E. *Org. Magn. Res.* **1981**, *17*, 250.
(48) The data can be obtained free of charge via the Internet at www.ccdc.cam.ac.uk/conts/retrieving.html or from the Cambridge Crystallographic Data Centre, 12 Union Road, Cambridge CB21EZ, U.K.; fax: (+44) 1223-336-033; or deposit@ccdc.cam.ac.uk.
(49) Köhn, F. Diploma Thesis, Universität Heidelberg, Heidelberg, Germany, 1998.
(50) Heister, K.; Zharnikov, M.; Grunze, M.; Johansson, L. S. O. *J. Phys. Chem. B* **2001**, *105*, 4058.
(51) Wirde, M.; Gelius, U.; Dunbar, T.; Allara, D. L. *Nucl. Instrum. Methods Phys. Res. B* **1997**, *131*, 245.
(52) Jäger, B.; Schrmann, H.; Müller, H. U.; Himmel, H.-J.; Neumann, M.; Grunze, M.; Wöll, Ch. *Z. Phys. Chem.* **1997**, *202*, 263.
(53) Heister, K.; Zharnikov, M.; Grunze, M.; Johansson, L. S. O.; Ulman, A. *Langmuir* **2001**, *17*, 8.
(54) Zharnikov, M.; Grunze, M. *J. Vac. Sci. Technol. B* **2002**, *20*, 1793.
(55) *Surface chemical analysis*—X-ray photoelectron spectrometers—Calibration of the energy scales, ISO 15472,2001.
(56) Moulder, J. F.; Stickle, W. E.; Sobol, P. E.; Bomben, K. D. *Handbook of X-ray Photoelectron Spectroscopy*; Chastian, J., Ed.; Perkin-Elmer Corp.: Eden Prairie, MN, 1992.
(57) Stöhr, J. *NEXAFS Spectroscopy*; Springer Series in Surface Science 25; Springer-Verlag: Berlin, 1992.
(58) Frey, S.; Heister, K.; Zharnikov, M.; Grunze, M.; Tamada, K.; Colorado, R., Jr.; Graupe, M.; Shmakova, O. E.; Lee, T. R. *Isr. J. Chem.* **2000**, *40*, 81.
(59) Zharnikov, M.; Frey, S.; Heister, K.; Grunze, M. *Langmuir* **2000**, *16*, 2697.
(60) Batson, P. E. *Phys. Rev. B* **1993**, *48*, 2608.
(61) March, J. In *Advanced Organic Chemistry*, 4th ed.; Wiley-Interscience: New York, 1992.
(62) Suzuki, H. *Electronic Absorption Spectra and Geometry of Organic Molecules*; Academic Press: New York, 1967.
(63) Nijegorodov, N. I.; Downey, W. S.; Danailov, M. B. *Spectrochim. Acta Part A* **2000**, *56*, 783.
(64) Wagner, P. J.; Scheve, B. J. *J. Am. Chem. Soc.* **1977**, *99*, 2888.
(65) Schweitzer, D.; Haenel, M. W. *Chem. Ber.* **1985**, *118*, 163.
(66) Gölzhäuser, A.; Panov, S.; Schertel, A.; Mast, M.; Wöll, Ch.; Grunze, M. *Surf. Sci.* **1995**, *334*, 235.
(67) Whelan, C. M.; Barnes, C. J.; Walker, C. G. H.; Brown, N. M. D. *Surf. Sci.* **1999**, *425*, 195.
(68) Whelan, C. M.; Smyth, M. R.; Barnes, C. J. *Langmuir* **1999**, *15*, 116.
(69) Heister, K.; Rong, H.-T.; Buck, M.; Zharnikov, M.; Grunze, M.; Johansson, L. S. O. *J. Phys. Chem. B* **2001**, *105*, 6888.
(70) Shaporenko, A.; Brunnbauer, M.; Terfort, A.; Johansson, L. S. O.; Grunze, M.; Zharnikov, M. *Langmuir* **2005**, *21*, 4370.
(71) Shaporenko, A.; Terfort, A.; Grunze, M.; Zharnikov, M. *J. Electron. Spectrosc. Relat. Phenom.*, in press.
(72) Laibinis, P. E.; Whitesides, G. M.; Allara, D. L.; Tao, Y.-T.; Parikh, A. N.; Nuzzo, R. G. *J. Am. Chem. Soc.* **1991**, *113*, 7152.
(73) Kondoh, H.; Iwasaki, M.; Shimada, T.; Amemiya, K.; Yokoyama, T.; Ohta, T.; Shimomura, M.; Kono, S. *Phys. Rev. Lett.* **2003**, *90*, 066102/1.
(74) Thome, J.; Himmelhaus, M.; Zharnikov, M.; Grunze, M. *Langmuir* **1998**, *14*, 7435−7449.
(75) Lamont, C. L. A.; Wilkes, J. *Langmuir* **1999**, *15*, 2037.
(76) Fuxen, C.; Azzam, W.; Arnold, R.; Witte, G.; Terfort, A.; Wöll, Ch. *Langmuir* **2001**, *17*, 3689.

(77) Zharnikov, M.; Grunze, M. *J. Phys. Condens. Matter*. **2001**, *13*, 11333.
(78) Shaporenko, A.; Adlkofer, K.; Johansson, L. S. O.; Tanaka, M.; Zharnikov, M. *Langmuir* **2003**, *19*, 4992.
(79) Horsley, J. A.; Stöhr, J.; Hitchcock, A. P.; Newbury, D. C.; Johnson, A. L.; Sette, F. *J. Chem. Phys.* **1985**, *83*, 6099.
(80) Yokoyama, T.; Seki, K.; Morisada, I.; Edamatsu, K.; Ohta, T. *Phys. Scr*. **1990**, *41*, 189.
(81) Weiss, K.; Gebert, S.; Wühn, M.; Wadepohl, H.; Wöll, Ch. *J. Vac. Sci. Technol., A* **1998**, *16*, 1017.
(82) Ågren, H.; Vahtras, O.; Carravetta, V. *Chem. Phys.* **1995**, *196*, 47.
(83) Rong, H. T.; Frey, S.; Yang, Y. J.; Zharnikov, M.; Buck, M.; Wühn, M.; Wöll, Ch.; Helmchen, G. *Langmuir* **2001**, *17*, 1582.
(84) Kitaigorodskii, I. A. *Organic Chemical Crystallography*; Consultants Bureau: New York, 1961.
(85) Cruickshank, D. W. J. *Acta Crystallogr*. **1956**, *9*, 915.
(86) Charbonneau, G.-P.; Delugeard, Y. *Acta Crystallogr*. **1976**, *B32*, 1420.
(87) Chang, S.-C.; Chao, I.; Tao, Y.-T. *J. Am. Chem. Soc*. **1994**, *116*, 6792.
(88) Dhirani, A.-A.; Zehner, W.; Hsung, R. P.; Guyot-Sionnest, P.; Sita, L. *J. Am. Chem. Soc*. **1996**, *118*, 3319.